

NASA-CR-197758

WING AND WING-BODY CONFIGURATIONS
ON PARALLEL COMPUTERS Final Report,
Feb. 1992 - Jan. 1995 (MCAT Inst.)
24 p

Unclas

MCAT Institute
Final Report
95-14

G3/05 0048495

Aeroelasticity of Wing and Wing-Body Configurations on Parallel computers

Chansup Byun



January 1995

NCC2-740

MCAT Institute
3933 Blue Gum Drive
San Jose, CA 95127

1000

1000

1000

1000

1000

1000

1000

1000

1000



**AEROELASTICITY OF WING AND WING-BODY
CONFIGURATIONS ON PARALLEL COMPUTERS**

**ORIGINAL CONTAINS
COLOR ILLUSTRATIONS**

Chansup Byun
MCAT Institute

Final Report For the Period of Time
February 1992 - January 1995
Co-operative Agreement : NCC2-740

January 1995

(BLANK PAGE)

AEROELASTICITY OF WING AND WING-BODY CONFIGURATIONS ON PARALLEL COMPUTERS

I. INTRODUCTION

There is a continuous effort to improve the performance of subsonic transport aircraft.¹ One attempt is to improve the fuel efficiency by extending the flight regime to high sub-transonic Mach numbers to increase lift-to-drag ratios and flight speeds. To avoid the high drag associated with strong shock waves, these advanced transports require modern wing sections such as supercritical wings that delay the shock wave formation. Early experiments have shown that these advanced wings experience an undesirable reduction in the flutter speed at the transonic regime. Such a phenomenon commonly known as 'transonic dip', is more pronounced for wings with supercritical airfoils.² Furthermore, for accurate prediction of the flutter characteristics, it is necessary to model viscous flows using the Navier-Stokes equations.

To date, advanced wing calculations have been limited to steady and unsteady computations on rigid wings. However, it is necessary to account for the structural flexibility to accurately compute its aeroelastic characteristics. The aeroelastic deformation resulting from this flexibility can significantly change the nature of the flow. Strong interactions between the flow and structures can lead to sustained aeroelastic oscillations for swept wings.³ Also, it is necessary to include the flexibility for proper correlations of computed data with experiments, particularly with those obtained from flight tests. To compute the flows accurately, it is necessary to include both aerodynamic and structural effects of the body. Recent efforts have been made to include the flexibility effects for wing-body configurations.⁴

Furthermore, in recent years, significant advances have been made for parallel computers in both hardware and software. Now parallel computers have become viable tools in computational mechanics. In order to exploit the new architecture of parallel computers, the computer code, ENSAERO,⁵ which computes the unsteady aerodynamics and aeroelasticity of aircraft by using the thin layer Navier-Stokes equations, has been parallelized on the Intel iPSC/860 parallel computer. The parallel version of the code has demonstrated its capability to compute aeroelastic responses by concurrently integrating the Euler equations and the structural equations of motion with aeroelastically deforming grids.⁶ The code can also model unsteady viscous flows using time-accurate, finite-difference schemes based on the Beam-Warming algorithm with the Baldwin-Lomax turbulence model.

The objective of this research is to develop computationally efficient methods for solving aeroelasticity problems on parallel computers. Both uncoupled and coupled methods are studied in this research. For the uncoupled approach, the conventional U-g method is

used to determine the flutter boundary. The generalized aerodynamic forces required are obtained by the pulse transfer-function analysis method. For the coupled approach, the fluid-structure interaction is obtained by directly coupling finite difference Euler/Navier-Stokes equations for fluids and finite element dynamics equations for structures. This capability will significantly impact many aerospace projects of national importance such as Advanced Subsonic Civil Transport (ASCT), where the structural stability margin becomes very critical at the transonic region. This research effort will have direct impact on the High Performance Computing and Communication (HPCC) Program of NASA in the area of parallel computing.

II. PREVIOUS STATUS

A multidisciplinary code for computing unsteady flows and aeroelastic responses of aerospace vehicles, ENSAERO, has been developed on serial supercomputers at the Applied Computational Aerodynamics Branch of the NASA Ames Research Center.⁷ This multidisciplinary code computes unsteady aerodynamic responses of aircraft using the Euler/Navier-Stokes equations. An aeroelastic shape-conforming moving grid is used to include the effect of structural deformations on unsteady flows. This code is designed in a modular fashion to adopt several different numerical schemes suitable for accurate aeroelastic computations. The basic coding of ENSAERO can accommodate zonal grid techniques for efficient modeling of full aircraft.

An early version of ENSAERO⁸ has been successfully applied in computing aeroelastic responses of a rectangular wing by using the Euler equations for fluids and the modal equations for structures. The result demonstrates that the code can accurately predict the flutter dynamic pressure of a rectangular wing. The code was extended to compute aeroelastic responses using the Navier-Stokes equations for fluids.⁹ Later, it was updated by utilizing an upwind algorithm, and the code has been applied to fighter wings undergoing unsteady motions^{10,11} at moderately large angles of attack. This code also has a capability of modeling moving control surfaces.¹² Furthermore, ENSAERO has demonstrated the capability to simulate transonic flows on wing-body configurations using the Navier-Stokes equations.¹³

In the past, the modal equations were used to model structures for the purpose of aeroelastic analysis. For simple geometries such as clean wings, the modal approach can predict accurate response results. However, the modal approach may be less accurate for complex structures such as wing-body configurations. In order to accurately represent aeroelastic responses of general wing-body configurations, the modal equations should be replaced with the finite element equations. Recently, a typical wing-body configuration has been used to demonstrate aeroelastic responses at transonic Mach numbers using

the Navier-Stokes equations for fluids and the finite element equations for structures.¹⁴ Simple one-dimensional beam elements are used to model the wing-body structures. Each node has three degrees of freedom (DOF) corresponding to transverse displacement and to transverse and torsional rotations, respectively.

Recently, a version of ENSAERO¹⁵ that uses the Euler equations for fluids and the modal equations for structures has been parallelized on the Intel iPSC/860 at Ames. The Intel iPSC/860 is a distributed-memory, multiple-instruction, multiple-data (MIMD) computer with 128 processors. In this parallel implementation, a domain decomposition approach is used in which the fluid equations and the structural equations are modeled in separate computational domains. Each domain is mapped individually onto a group of processors, referred to as a cube on the Intel iPSC/860. However, because of the coupling between the disciplines, there is a need to exchange data, such as pressures and structural deformations at interfaces. This exchange between the fluid and structural domains is accomplished through an intercube communication mechanism,¹⁶ which enables different processors in each cube to communicate directly.

III. CURRENT WORK

1. FINITE ELEMENT MODELING OF STRUCTURES

The finite element representation of structures generally provides more accurate modeling of structures than the modal representation does in aeroelastic computations. For the aeroelastic computations of wing and wing-body structures, plate and shell models are used as reported in References 4 and 17. The parallel implementation of the structural domain is mainly discussed in Ref. 17. Although the current implementation is only using ANS4 plate/shell elements to model structures, it is possible to use different types of elements.

2. FLUID-STRUCTURAL INTERFACE

In aeroelastic analysis, it is necessary to represent the equivalent aerodynamic loads at the structural nodal points and to represent the deformed structural configurations at the aerodynamic grid points. In the present domain decomposition approach, coupling between the fluid and structural domains is achieved by interfacing the boundary data, such as aerodynamic pressures and structural deflections, at each time step. An analytical moving-grid technique has been successfully used to deform the aerodynamic grid according to the structural deflections at the end of every time-step.^{7,8,14} There are different approaches for obtaining the external load vector, depending on the equations used for the structural dynamic analysis.

In order to replace modal equations with finite element structural dynamics equations for fluid-structural interaction problems, a new fluid-structural interface, similar to the modal matrix used for modal equations, should be developed. Several numerical procedures have been developed for exchanging the necessary information between the fluid and structural domains.¹⁸⁻²⁰ In this research, two different types of fluid-structural interfaces were studied and compared as shown in Ref. 4.

The current implementation of the fluid-structural interface on the Intel iPSC/860 is based on direct node-to-node communication. Thus each of processors assigned to the fluid domain can communicate with any processors of the structural domain. A typical communication pattern is generally irregular during the aeroelastic computation of a High Speed Civil Transport (HSCT) model on the Intel iPSC/860. More details are found in Ref. 6.

3. PARALLEL INTEGRATION

In a serial computer, the integration of both fluid and structural equations is performed one after the other in a sequential nature. When implementing the integration scheme on parallel computers, all processors can be used to solve the fluid and structural equations sequentially. But this approach requires more memory per processor and two disciplines have to be implemented in a single program. As a result, modularity of each algorithm for individual disciplines will have to be sacrificed to a significant degree. In addition, this approach will be less efficient as increasing the number of processors because the problem is not linearly scaled.

However, while keeping modularity of each discipline, computations can be done more efficiently on MIMD parallel computers by executing the integration of both fluid and structural equations concurrently. In the proposed parallel integration scheme, both domains start computations independently and one of the solvers waits until the other finishes its calculation. Then they exchange the required data with each other for the next time step. By doing so, the parallel integration can reduce the idle time since only one cube (the fastest) will have to wait. This integration scheme exploits the parallelism offered by the domain decomposition approach to solve the coupled fluid-structural interaction problems. More details are found in Ref. 6 and 17.

4. STATIC AEROELASTICITY

It is of interest to find static deflections of aerospace vehicles subjected aerodynamic loads. In the past, static equilibrium equations of structures are used in ENSAERO to find the static deflections in conjunction with the aerodynamic forces computed by spacially variable time method starting from the steady state flow solutions as initial conditions. This method, however, shows highly oscillatory behavior in the solutions. Sometimes this

approach becomes highly unstable and difficult to obtain solutions. In order to overcome these problems, dynamic equilibrium equations with high damping are suggested to replace the static equilibrium equations of structures.²¹ The matrix form of the dynamic equilibrium equations of motion is

$$[M]\{\ddot{q}\} + [G]\{\dot{q}\} + [K]\{q\} = \{Z\} \quad (1)$$

where $[M]$, $[G]$, and $[K]$ are the mass, damping and stiffness matrices, respectively. $\{Z\}$ is the aerodynamic force vector. By adding the inertia and damping terms, the variation of displacements becomes smooth and the final solution approaches to the static equilibrium position of structures. This approach can start from the free stream conditions and obtain the steady state flow solution at the deformed configuration in addition to the static deflections. Furthermore, as pointed out in Ref. 21, this approach is quite stable and efficient compared to the previous approach. This method has been implemented in the current parallel version of ENSAERO.

5. FORMULATION FOR FLUTTER BOUNDARY PREDICTION

The direct coupling approach requires unprecedented amount of computation time to determine the flutter boundary in the past. Thus uncoupled approaches have been widely used to determine the flutter boundary. One of the uncoupled approaches is the U-g method, which computes the flutter speed by solving an eigenvalue problem. Following the Ref. 22, the eigenvalue equations can be derived as

$$[K]^{-1}[[M] + C[Q]]\{\bar{q}\} = \lambda\{\bar{q}\}$$

$$C = \frac{\rho c^3}{2k^2} \quad (2)$$

$$\lambda = \frac{(1 + ig)}{\omega^2}, \text{ complex eigenvalue}$$

where the reduced frequency, $k = \omega c/U$, c is the reference chord, and U is the flight speed. The generalized aerodynamic forces are obtained as

$$Q_{ij} = \frac{1}{c} \int \int h(x, y)_i \Delta C_p(x, y)_j dx dy \quad (3)$$

$$h = \text{modal displacement}$$

where i and j represent mode shapes. The coefficient Q_{ij} represents the force acting in the i^{th} mode due to pressure generated by the unsteady motion of the j^{th} mode and is dependent on the reduced frequency. For each reduced frequency chosen, the generalized aerodynamic force matrix $[Q]$ is obtained by solving the unsteady flow equations and then,

in turn, the complex eigenvalue problem can be solved to obtain the damping coefficient, g . The damping coefficient, g , is used to determine the flutter point.

One way to compute GAFs is the time integration (TI) approach. The TI method performs several cycles of a forced harmonic oscillation and uses the last cycle of oscillation to determine the first harmonic component of GAFs. Multiple unsteady computations are required at various reduced frequencies to generate GAFs for each structural mode used in the flutter analysis. Typically unsteady data at 3 to 4 given frequencies are required to make a reasonable prediction of the flutter point at a given flight speed when using the U-g method. Interpolation techniques are usually used to obtain the generalized aerodynamic forces at various reduced frequencies to accurately determine the flutter point. Although there have been great advances in conventional and parallel supercomputers, it is still formidable task to determine the flutter boundary using the time integration approach.

Repetitive computations of GAFs for each frequency can be avoided by using the indicial approach²³ or pulse transfer-function analysis (PTFA) method.^{24,25,26} In these approaches, GAFs for all frequencies for a given structural mode can be extracted from a single unsteady response computation. These approaches require an assumption that the unsteady flow can be linearized about a nonlinear steady flow. Such an assumption is valid for small perturbation. It is noted that classical flutter starts as a small perturbation phenomenon and, therefore, it is considered to be appropriate to use these approaches to make preliminary prediction of the flutter boundary.

The indicial method computes GAFs from the Fourier transform of the indicial response. That is, a step change in the structural mode is used as the initial condition and the unsteady computation is continued until the transient had decayed. The PTFA method is a variation of the indicial method. The Fourier transform of the resulting force response is divided by the transform of the generalized displacement of the given structural mode to obtain GAFs. It uses a forced modal motion represented by a smoothly varying pulse function instead of a step function. Both approaches can significantly reduce the computation time to generate GAFs compared to the time integration method. In this work, the generalized aerodynamic force matrix is computed by using both time integration and pulse transfer-function methods for comparison. However, the PTFA method is used to determine the flutter boundary.

6. PARALLELIZATION OF FLUTTER BOUNDARY PREDICTION

For the U-g method used to determine the flutter boundary, the generalized aerodynamic force matrix $[Q]$ is required as functions of the reduced frequency. Although the U-g method is an efficient method to determine the flutter boundary, it would become a CPU-intensive procedure when generalized aerodynamic forces (GAFs) are computed by

solving the Euler or Navier-Stokes unsteady flow equations instead of simplified unsteady aerodynamic equations. So the parallelization is concentrated on computing GAFs.

The parallelization of the flutter boundary prediction procedure can be achieved in three different ways. The first is the concurrent execution of unsteady computations associated with different structural mode shapes. This is represented as a box with broken line in Fig. 1. This computation can be accomplished for a fluid grid which fits on a single processor node. Upon completing unsteady computations, the generalized aerodynamic force matrix can be assembled with the minimal communication among processors assigned to a given flight condition. Then the flutter point can be determined from the eigenvalue analysis. This can be repeated for several flight Mach numbers to obtain the flutter boundary. This is a coarse grain parallelization since parallelization is accomplished only for the given number of modal motions.

The second is the concurrent multiple execution of the first case with different initial steady-state conditions, e.g. different Mach numbers. Each column in Fig. 1 represents the first approach and the multiple columns represent the execution of the multiple unsteady flow analyses in parallel. In this way, the flutter boundary for the given flight regime can be determined in a single run. Upon completion of unsteady modal motion, the pulse transfer-function analysis yields GAFs as functions of the reduced frequency. Flutter points can be determined independently by solving the eigenvalue equations for various reduced frequencies after assembling the GAFs. In order to assemble GAFs, communication for unsteady data should be limited only among the processors with the same initial condition. This is accomplished by using the MPIRUN,²⁷ a utility developed at NASA Ames Research Center. The MPIRUN enables to flexibly define a group of processors and communicate data within a group or between groups. The MPIRUN is based on the message passing interface (MPI) standard.²⁸

However, since each unsteady computation is still quite CPU-intensive task, it is not easy to complete the whole simulation in a single run. Therefore, in order to cut down the total run time, it is necessary to parallelize each unsteady flow computation. This parallelization is also necessary for bigger problems where the fluid grid can not fit on a single processor node. This involves the parallelization of the flow solver and the moving grid scheme. This is referred to a fine grain parallelization. It requires another level of communication so that each modal motion can be subdivided and distributed onto M number of processors as shown in Fig. 1. Thus, during the solution stage of unsteady flow equations, communication should be limited among the processors with the same forced modal motion and the initial condition. More details for parallelization of the flow solver on the Intel iPSC/860 computer can be found in Reference 29. The allocation of processor nodes is determined by the number of vibration modes selected, the size of the

computational grid, and the number of cases for different flight speeds. By combining the above three approaches together, the procedure can determine the flutter boundary for a given wing with significant reduction in computational time.

7. COMPUTATIONAL RESULTS

a. Dynamic Aeroelasticity

Dynamic aeroelastic computations for the NASA Langley Clipped Delta Wing were performed first on a Cray Y-MP serial computer and then on the Intel iPSC/860 MIMD parallel computer. Comparison between the modal and finite element analyses for structures and accuracy of the interfaces considered in this research are given in Ref. 4.

Computational performance results are found in Ref. 17. Including the data exchange between fluid and structural domains, the current aeroelastically deforming grid scheme requires about 12 percent of the computational time per each integration step.

Application of the procedure to wing-body configurations can be found in Ref. 4 and 6. Dynamic aeroelastic computations are done on flexible wing and body structures such as a simple wing-body and a Boeing 1807 HSCT model. The results are given in Ref. 6.

b. Static Aeroelasticity

For demonstration purpose of static aeroelasticity, the LANN wing was selected since this wing represent the ASCT type wing configuration. The LANN model has an aspect ratio of 7.92, a taper ratio of 0.40 and a leading-edge sweep angle of 27.5 degrees. The airfoil sections are supercritical with constant thickness-to-chord ratio of 12 percent. This model was tested in the transonic wind tunnel (HST), the Netherlands. Details of steady flow measurements are given in Ref. 30.

Computations are made using the built-in C-H grid topology available in the EN-SAERO code. For the flow computations, a grid of size $151 \times 35 \times 35$ (151 points in streamwise direction, 35 points in both spanwise and surface-normal directions) is selected as it was found to be appropriate for this problem in the early work.³¹ Using this grid, a steady computation is made at $M = 0.87$, $Re = 7.6 \times 10^6$ degrees and $AoA = 3.0$. As shown in Fig. 2, it is also noted that, the Euler equations did not properly represent the flow over the LANN wing. This figure shows that the Navier-Sokes equations with the Baldwin-Lomax turbulence model obtained the result in good agreement with the experiment. It is of interest to investigate the effect of viscosity on the static deflection.

Figure 3 shows surface pressure distributions obtained using the Navier-Stokes equations at the same free stream condition. The effect of viscosity is shown at Fig. 4. For

this particular problem, the leading edge deflection of the wing computed by using the Navier-Stokes equations are smaller than that obtained by using the Euler equations.

Figures 5 and 6 shows the effect of flexibility on pressure distributions. Both figures show quite different trends when the wing is allowed to be flexible. For the Euler computations, the shock on the upper surface moves forward to the leading from the rigid solution whereas, for the Navier-Stokes computations, the shock position moved backward from the rigid solution. Figure 7 shows the surface pressure distributions at the deformed configurations.

c. Parallel Flutter Boundary Prediction

In order to validate the present procedure and compare the pulse transfer-function analysis (PTFA) method with the time integration (TI) method, computations were made for a unswept rectangular wing of aspect ratio 5 with a 6% thick circular-arc airfoil.³¹ The model is 11.50 in. in the spanwise direction and in the 4.56 in. chordwise direction. The transonic flutter characteristics of this wing are available from wind tunnel tests for various flow parameters. For this computation, the flow field is solved using the Euler equations with a C-H grid of size $151 \times 25 \times 30$.

Generalized Aerodynamic Forces

To compare the PTFA method with the TI method, the unswept rectangular wing was selected. The first three structural modes are used in the flutter analysis. The maximum amplitude of the generalized displacements is controlled to be small enough so that the response of the aerodynamic forces is linear. All computations were made on the Cray C90 computer for the purpose of comparison between the TI and PTFA methods. For the TI method, the unsteady data is obtained by integrating the unsteady flow equations when the wing is oscillating in harmonic motion for a given structural mode. The TI method required three cycles with 3600 time steps per cycle for a complete calculation. This computation required about 2 CPU hours on a single Cray C-90 processor. Using the PTFA method, the unsteady data are obtained by perturbing the wing with a smoothly varying pulse input for a given structural mode. The total CPU time required for a single PTFA run is about 1.5 hours on a single Cray C-90 processor. It should be noted that the unsteady computation has to be continued until the transient has decayed.

Figures 8 and 9 show the lift coefficient history obtained by using the TI and PTFA methods, respectively. Both results are obtained from unsteady computations by using the Euler equations at free stream Mach 0.715 and zero angle of attack. For the TI method, since a harmonic motion is enforced, the residual shows that the transient dies out and the lift coefficient show periodicity in response as shown in Fig. 8. Since a pulse motion is enforced for the PTFA method, there is no periodicity in response as shown in Fig.

9. However, the lift coefficient response from the PTFA method shows that the transient due to the pulse motion has decayed out and the solution converged to the steady-state condition.

The comparison of the GAFs obtained using the TI and PTFA methods is presented in Fig. 10. The results are obtained for the unswept rectangular wing at the free stream Mach 0.715 and zero angle of attack by using the Euler flow equations. Both results show in good agreement. It was observed in the past that the results from the PTFA method became deviated from the results obtained by the TI method as increasing the reduced frequency.³³ However, as shown in Fig. 10, it is considered that the PTFA is applicable to generate GAFs within the range of the reduced frequency required for the flutter prediction.

Flutter Determination

The present flutter prediction procedure has been validated by comparing the computational results with the experiment. The comparison between the results from the computation and experiment is made in the Fig. 11. The computed flutter frequencies are compared with those obtained in the experiment. The computational results show similar trend as compared to the experiment at the lower Mach number range although the computed result predicts the transonic dip earlier than the experiment. The difference in the prediction of the transonic dip can be attributed to the possible viscous effect since the Euler equations are used in the computation.

IV. SUMMARY AND CONCLUSIONS

In this work, procedures to compute aeroelastic responses of wing and wing-body structures have been parallelized on MIMD parallel computers using uncoupled and coupled approaches. For the coupled approach, dynamic aeroelastic responses are obtained by direct coupling of the finite difference Euler/Navier Stokes equations for fluids and the finite element dynamics equations for structures for wing and wing-body structures. The procedure is based on a domain decomposition approach which enables algorithms for the fluid and structural disciplines to be developed and maintained independently.

A parallel integration procedure is developed to solve fluid and structural equations together. The parallel integration scheme enables the combination of advanced CFD and CSD technologies with minimal increase in computational time per integration step while keeping modularity of each discipline. The time per integration step is solely determined by the domain that requires most computational time on the iPSC/860. This parallel integration is one of the advantages of using MIMD computers for multidisciplinary analysis. The procedure developed in this research will provide an efficient tool for solving aeroelastic problems of complete aerospace vehicle configurations on MIMD computers.

For the uncoupled approach, the conventional U-g method is used to determine the flutter boundary. Current implementation of the proposed procedure for the flutter prediction using the U-g method is limited to coarse grain parallelization. Thus the flow solver is running on a single node and several flow conditions and oscillating modes are executed simultaneously.

Based on this work the following conclusions can be made.

1. It is feasible to directly couple the finite difference flow equations and finite element structural equations to obtain accurate results, though each discipline is solved in a separate computational domain. This domain decomposition approach takes advantage of efficient methods developed for each individual discipline. This approach can be extended to include more other disciplines, e.g., controls, optimizations, etc.
2. The use of pulse transfer-function method for generalized aerodynamic forces (GAFs) is suitable for the problems solved in this work. This method is very efficient to obtain GAFs as a function of the reduced frequency.
3. The parallel procedure for the prediction of the flutter boundary can obtain the flutter boundary in efficient manner on MIMD parallel computers.

ACKNOWLEDGMENTS

This work was completed using the resources of the Numerical Aerodynamic Simulation (NAS) Program at NASA Ames Research Center. The work was funded through NASA Ames Research Center Cooperative Agreement Number NCC2-740 under the HPCC program.

REFERENCES

1. Goldhammer, M. I. and Steinle, F. W., "Design and Validation of Advanced Transonic Wings Using CFD and Very High Reynolds Number Wind Tunnel Testing," ICAS 90-2.6.2, 17th Congress, Stockholm, Sweden, Sept. 9-14, 1990.
- ✓2. Farmer, M. G., Hanson, P. W. and Wynne, E. C., "Comparison of Supercritical and Conventional Flutter Characteristics," NASA TM X-72837, May 1976. *OK*
3. Guruswamy, G. P., "Vortical Flow Computations on a Flexible Blended Wing-Body Configuration," *AIAA J.*, Vol. 30, No. 10, Oct. 1992, pp. 2497-2503.
4. Guruswamy, G. P. and Byun, C., "Fluid-Structural Interactions Using Navier-Stokes Flow Equations Coupled with Shell Finite Element Structures," AIAA Paper 93-3087, July 1993.

5. Guruswamy, G. P., "ENSAERO-A Multidisciplinary Program for Fluid/Structural Interaction Studies of Aerospace Vehicles," *Computing System Engineering*, Vol. 1, Nos. 2-4, 1990, pp. 237-256.
6. Byun, C. and Guruswamy, G. P., "Wing-Body Aeroelasticity Using Finite-Difference Fluid/ Finite-Element Structural Equations on Parallel Computers," AIAA Paper 94-1487, April 1994.
7. G. P. Guruswamy, "ENSAERO - A Multidisciplinary Program for Fluid/ Structural Interaction Studies of Aerospace Vehicles," *Computing Systems Engineering*, Vol. 1, 1990, pp. 237-256.
8. G. P. Guruswamy, "Unsteady Aerodynamic and Aeroelastic Calculations for Wings Using Euler Equations," *AIAA J.*, Vol. 28, 1990, pp. 461-469.
9. G. P. Guruswamy, "Navier-Stokes Computations on Swept-Tapered Wings, Including Flexibility," AIAA Paper 90-1152, Apr. 1990.
10. S. Obayashi, G. P. Guruswamy and P. M. Goorjian, "Application of Streamwise Upwind Algorithm for Unsteady Transonic Computations over Oscillating Wings," AIAA Paper 90-3103, Aug. 1990.
11. S. Obayashi and G. P. Guruswamy, "Unsteady Shock-Vortex Interaction on a Flexible Delta Wing," AIAA Paper 91-1109, Apr. 1991.
12. S. Obayashi and G. P. Guruswamy, "Navier-Stokes Computations for Oscillating Control Surface," AIAA Paper 92-4431, Aug. 1992.
13. S. Obayashi, G. P. Guruswamy and E. L. Tu, "Unsteady Navier-Stokes Computations on a Wing-Body Configuration in Ramp Motions," AIAA Paper 91-2865, Aug. 1991.
14. G. P. Guruswamy, "Coupled Finite-Difference/Finite-Element Approach for Wing-Body Aeroelasticity," AIAA Paper 92-4680, Sep. 1992.
15. G. P. Guruswamy, S. Weeratunga and E. Pramono, "Direct Coupling Approach to Fluids/Structures Interaction Problems for Parallel Computing," NASA CAS Conference, Moffett Field, CA 94035, Aug. 18-20, 1992, pp. 46-47.
16. E. Barszcz, "Intercube Communication on the iPSC/860," Proceedings of the Scalable High Performance Computing Conference, Williamsburg, VA, April 26-29, 1992, pp. 307-313.
- OK ✓ 17. Byun, C. and Guruswamy, G. P., "A Comparative Study of Serial and Parallel Aeroelastic Computations of Wings," NASA TM-108805, January 1994.
18. R. L. Harder and R. N. Desmarais, "Interpolation Using Surface Spline," *J. of Aircraft*, Vol. 9, 1972, pp. 189-191.
19. K. Appa, "Finite-Surface Spline," *J. of Aircraft*, Vol. 26, 1989, pp. 495-496.

20. R. M. V. Pidaparti, "Structural and Aerodynamic Data Transformation Using Inverse Isoparametric Mapping," *J. of Aircraft*, Vol. 29, 1992, pp. 507-509.
21. Shigeru Obayashi and Guruswamy, G. P., "Convergence Acceleration of an Aeroelastic Navier-Stokes Solver", AIAA Paper 94-2268, 25th AIAA Fluid Dynamics Conference, Colorado Springs, CO, June 20-23, 1994.
- ✓ 22. Desmarais, R. N. and Bennett, R. M., "User's Guide for a Modular Flutter Analysis software System (FAST Version 1.0)," NASA TM-78720, May 1978.
23. Ballhaus, W. F. and Goorjian, P. M., "Computation of Unsteady Transonic Flow by Indicial Method," *AIAA Journal*, No. 2, Vol. 16, Feb. 1978, pp. 117-124.
24. Lee-Rausch, E. M. and Batina, J. T., "Calculation of AGARD Wing 445.6 Flutter Using Navier-Stokes Aerodynamics," AIAA-93-3476, 11th Applied Aerodynamics Conf., Monterey, CA, Aug. 1993.
25. Seidel, D. A., Bennett, R. M. and Whitlow, W. Jr., "An Exploratory Study of Finite Difference Grids for Transonic Unsteady Aerodynamics," AIAA-83-0503, AIAA 21st Aerospace Sciences Meeting, Reno, Nevada, Jan. 10-13, 1983.
26. Bland, S. R. and Edwards, J. W., "Airfoil Shape and Thickness Effects on Transonic Airloads and Flutter," AIAA-83-0959, May 1983.
27. Feinberg, S., "MPIRUN: A Loader for Multidisciplinary and Multizonal MPI Applications," *NAS News*, Vol. 2, No. 6, Nov. Dec. 1994.
28. Message Passing Interface Forum, MPI: A Message-Passing Interface Standard, University of Tennessee, May 1994.
29. Ryan, J. S. and Weeratunga, S. K., "Parallel Computation of 3-D Navier-Stokes Flowfields for Supersonic Vehicles," AIAA Paper 93-0064, Jan. 1993.
30. Horsten, J. J., den Boer, R. G. and Zwaan, "Unsteady Transonic Pressure Measurements on a Semispan Wind Tunnel Model of A Transport Type Supercritical Wing, Part I General Description, Aerodynamic Coefficients and Vibration Modes," AFWAL-TR-83-3039, Air Force Wright Aeronautical Laboratories, April 1982.
31. Guruswamy, G. and Tu, E., "Navier-Stokes Computations on Flexible Advanced Transport-Type Wing Configurations in Transonic Regime," AIAA Paper 94-1725, April 1994.
- 0✓ 32. Dogget, R. V., Rainey, A. G. and Morgan, H. G., "An Experimental Investigation of Aerodynamics Effects of Airfoil Thickness on Transonic Flutter Characteristics," NASA TM X-79, 1959.
33. Seidel, D. A., Bennett, R. M. and Whitlow, W. Jr., "An Exploratory Study of Finite Difference Grids for Transonic Unsteady Aerodynamics," AIAA-83-0503, AIAA 21st Aerospace Sciences Meeting, Reno, Nevada, Jan. 10-13, 1983.

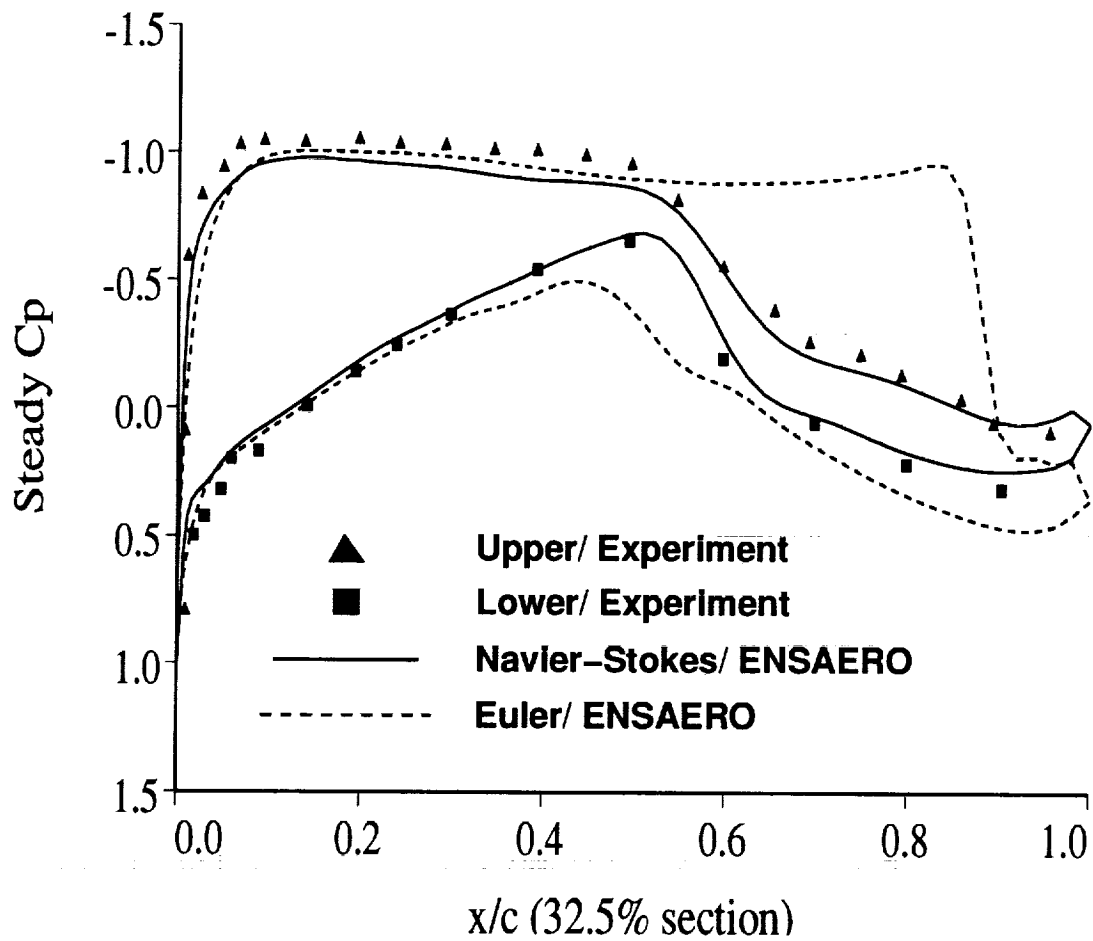
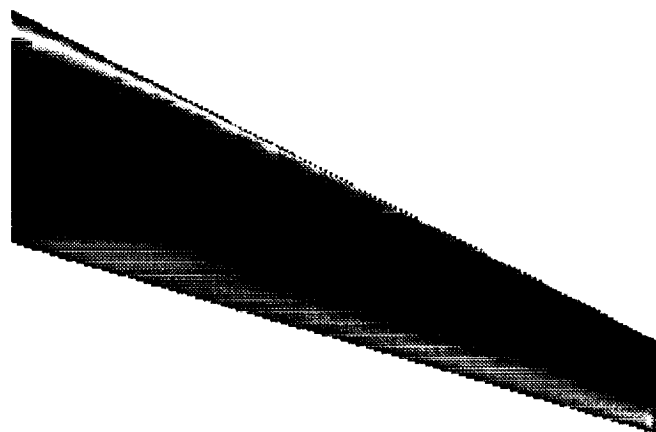


Figure 1. Comparison of sectional pressure coefficients among the computations and experiment at the freestream condition of $M = 0.871$, angle of attack 3.0 degrees, Reynolds number 7.472 million. (Code : ENSAERO, Grid : $151 \times 35 \times 35$)

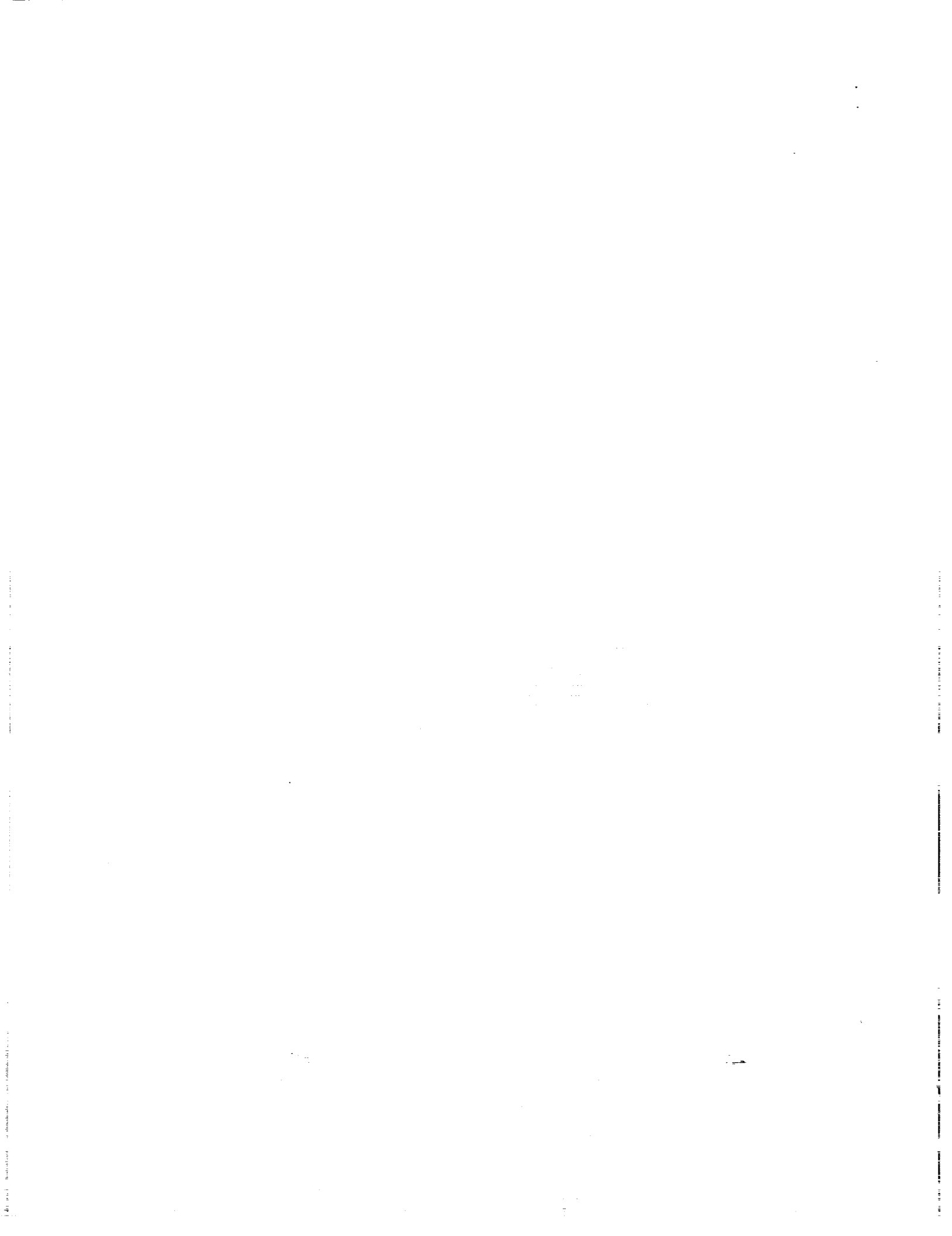


Upper surface



Lower surface

Figure 2. Surface pressure distributions obtained using Navier- Stokes equations at the freestream condition of $M = 0.871$, angle of attack 3.0 degrees, Reynolds number 7.472 million. (Code : ENSAERO, Grid : 151x35x35)



ORIGINAL PAGE
COLOR PHOTOGRAPH

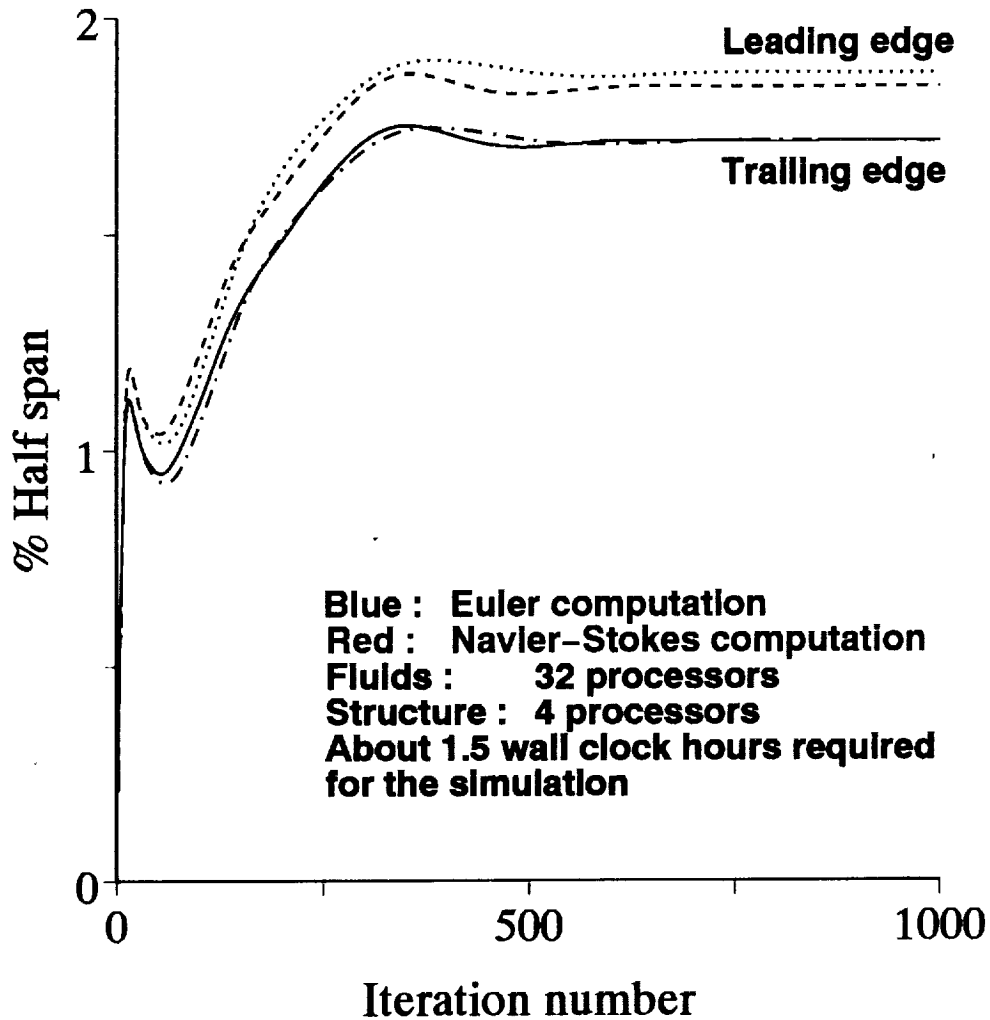
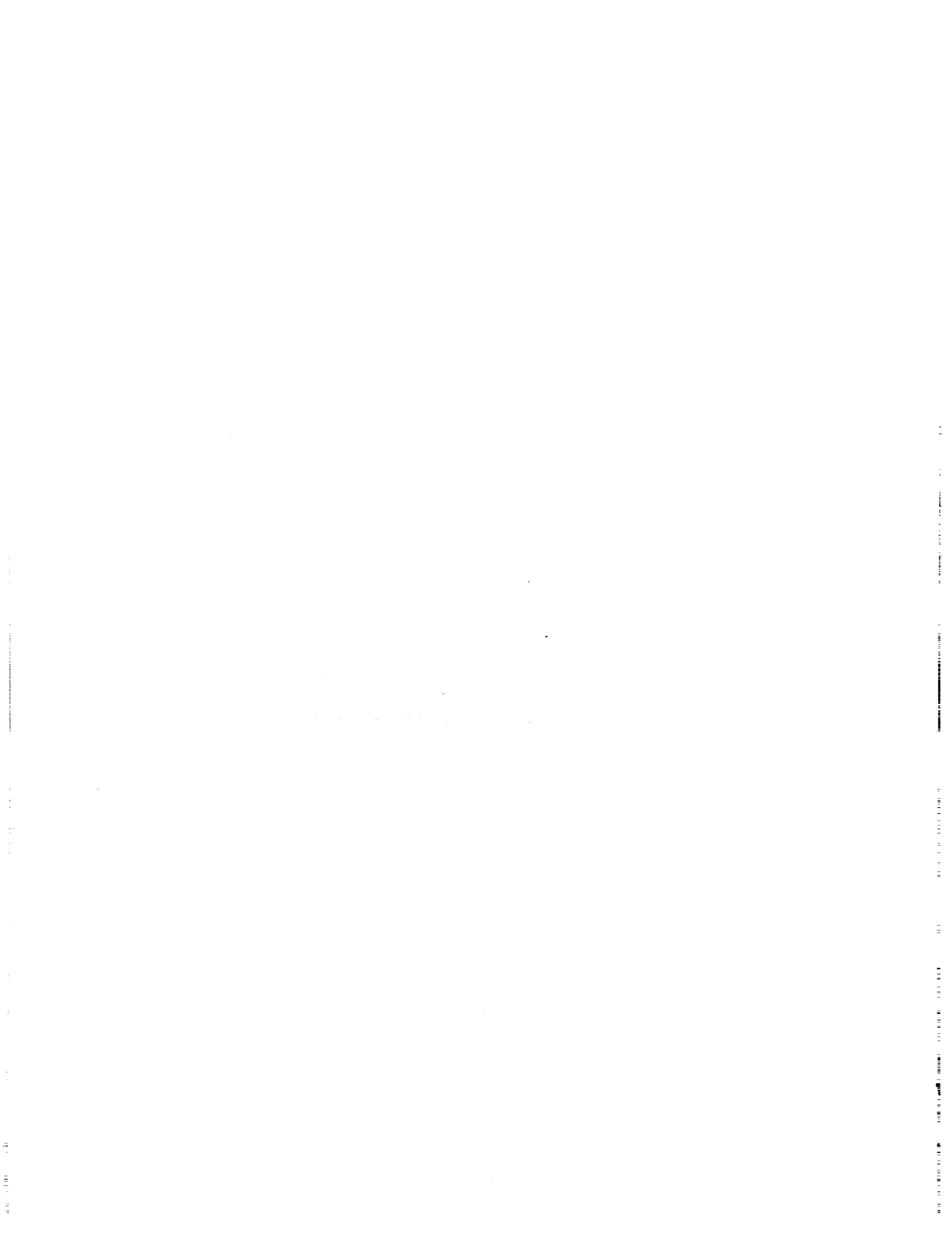


Figure 3. Effect of viscosity on static aeroelastic responses computed by directly coupling the Navier-Stokes flow equations with finite element structural dynamics equations on the Intel iPSC/860 computer (36 processors). (CFD Grid : 151x35x35, FE model : 128 plate elements)



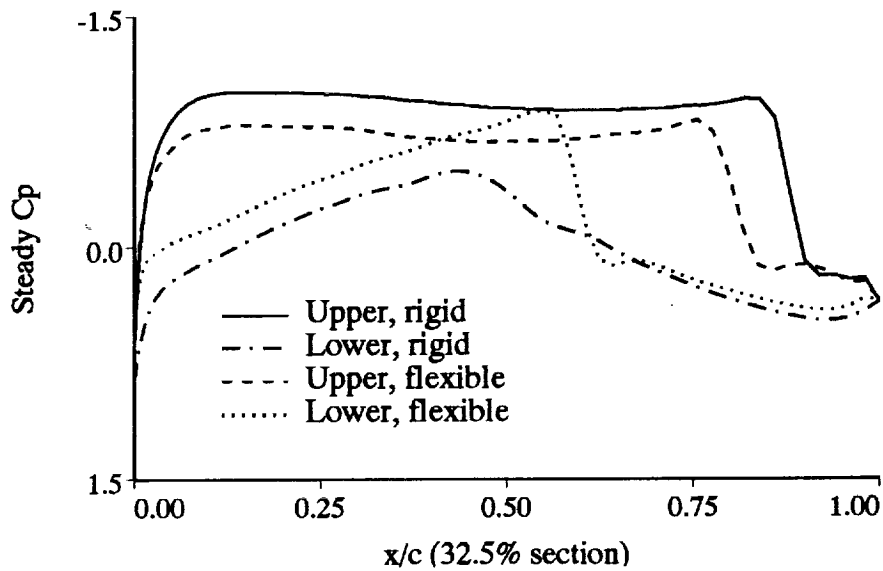


Figure 4. Effect of flexibility on pressure distributions of steady state solutions obtained by using the Euler equations. (CFD Grid : 151x35x35, FE model : 128 plate elements)

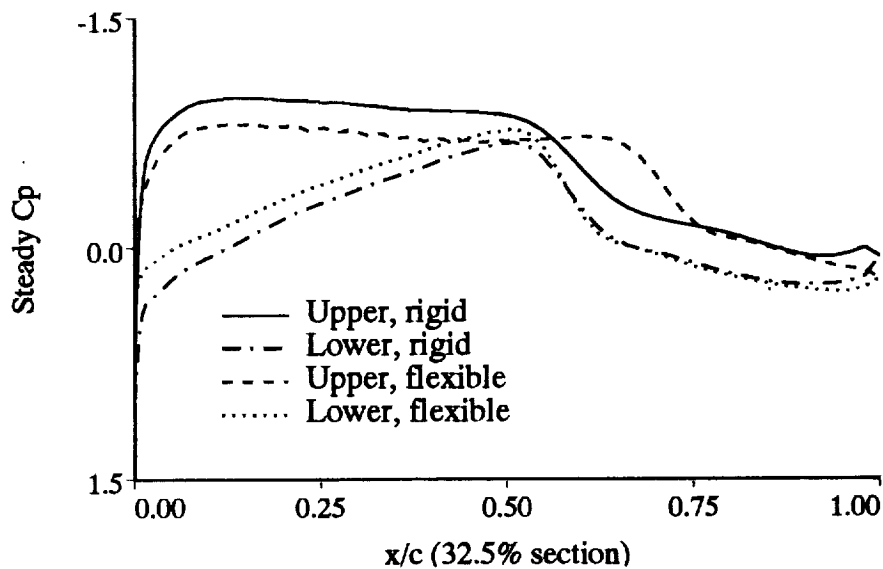
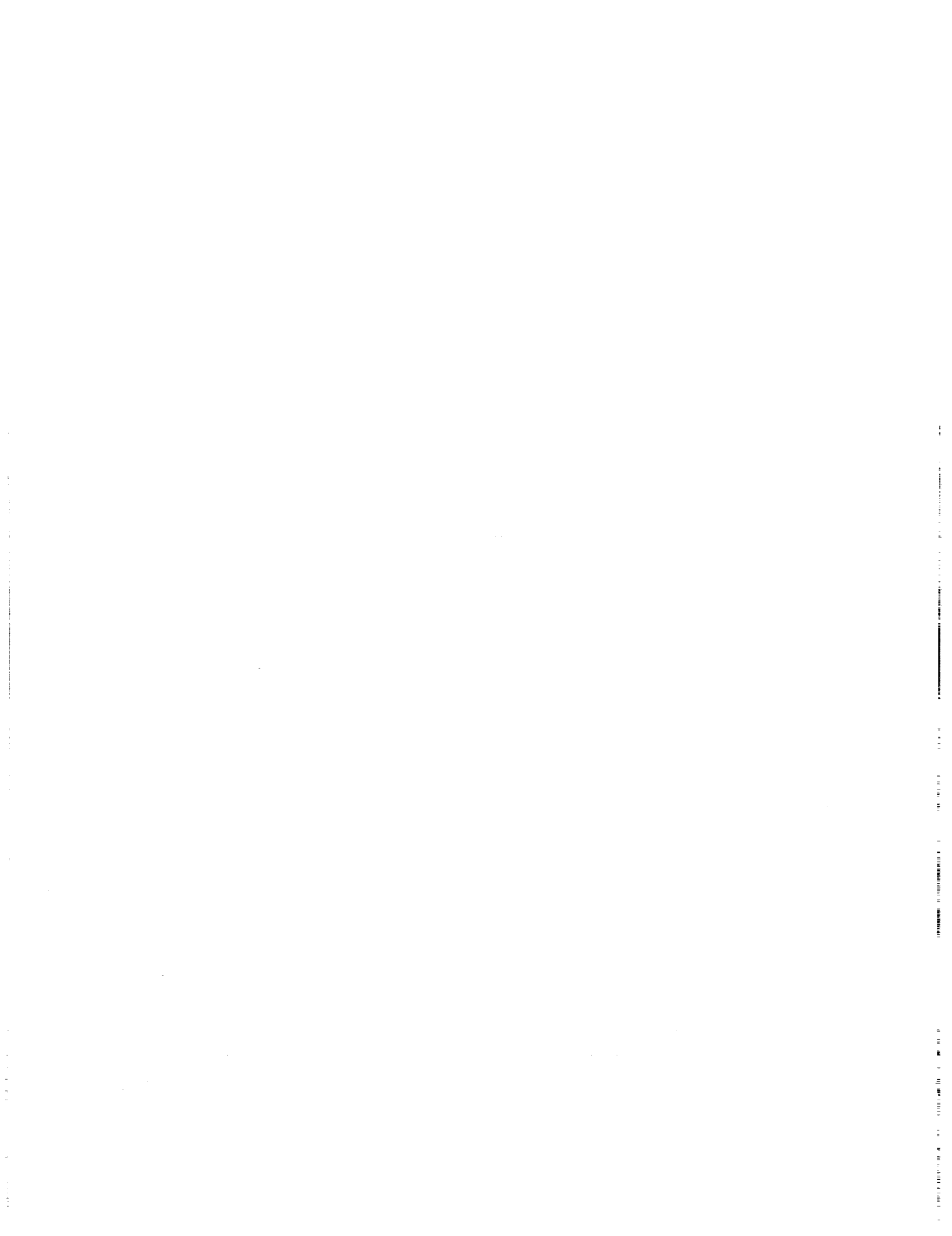


Figure 5. Effect of flexibility on pressure distributions of steady state solutions obtained by using the Navier-Stokes equations. (CFD Grid : 151x35x35, FE model : 128 plate elements)





Euler computation



Navier-Stokes computation

Figure 6. Surface pressure distributions on deformed configurations obtained at the freestream condition of $M = 0.871$, angle of attack 3.0 degrees, Reynolds number 7.472 million. (Code : ENSAERO, Grid : 151x35x35)

1. The first part of the document discusses the importance of maintaining accurate records of all transactions and activities. It emphasizes the need for transparency and accountability in financial reporting.

2. Key Findings

The analysis reveals several critical areas for improvement, including the need for enhanced internal controls and more frequent audits.

It is recommended that the organization implement a robust risk management framework to identify and mitigate potential threats to its operations.

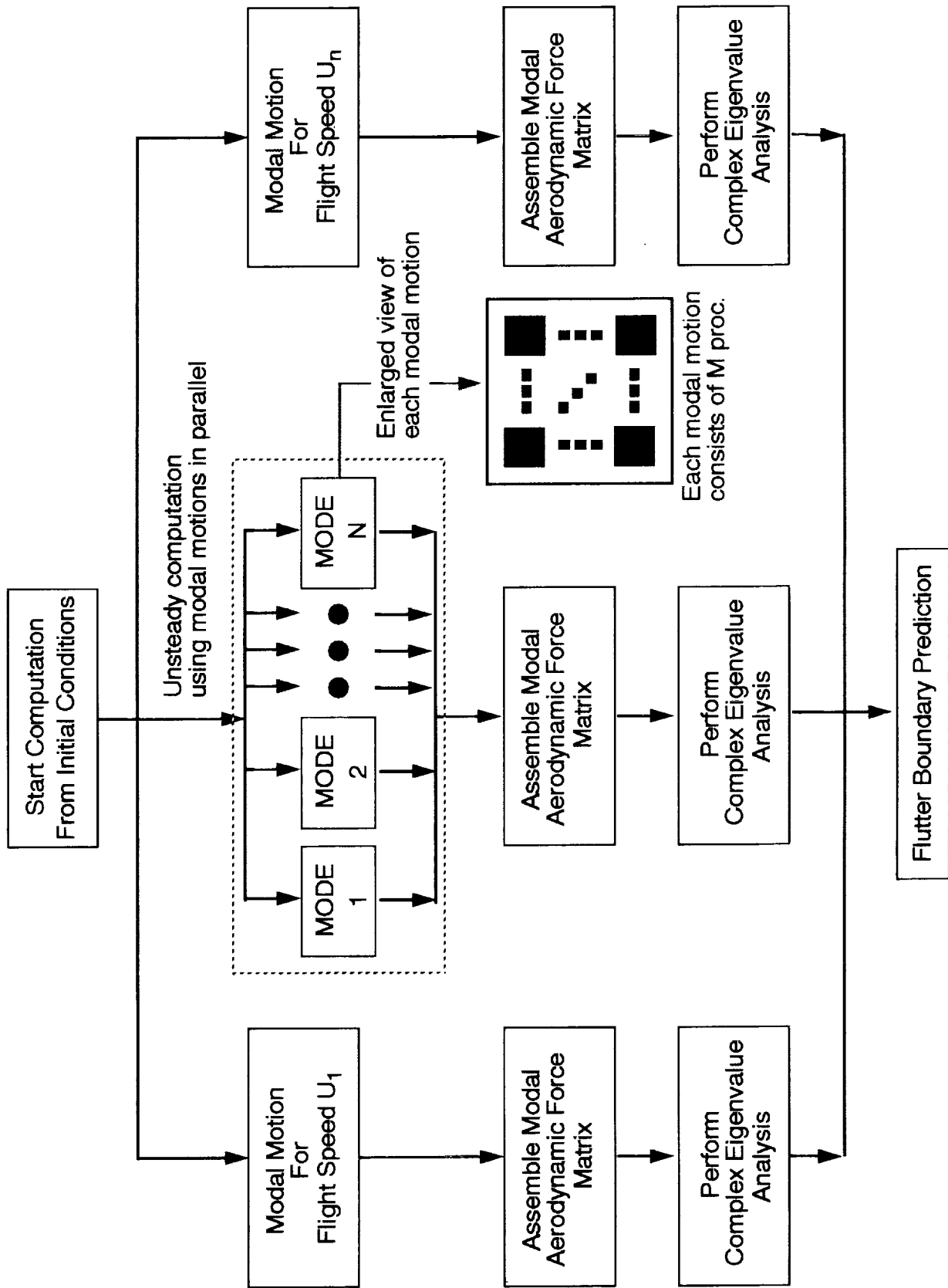
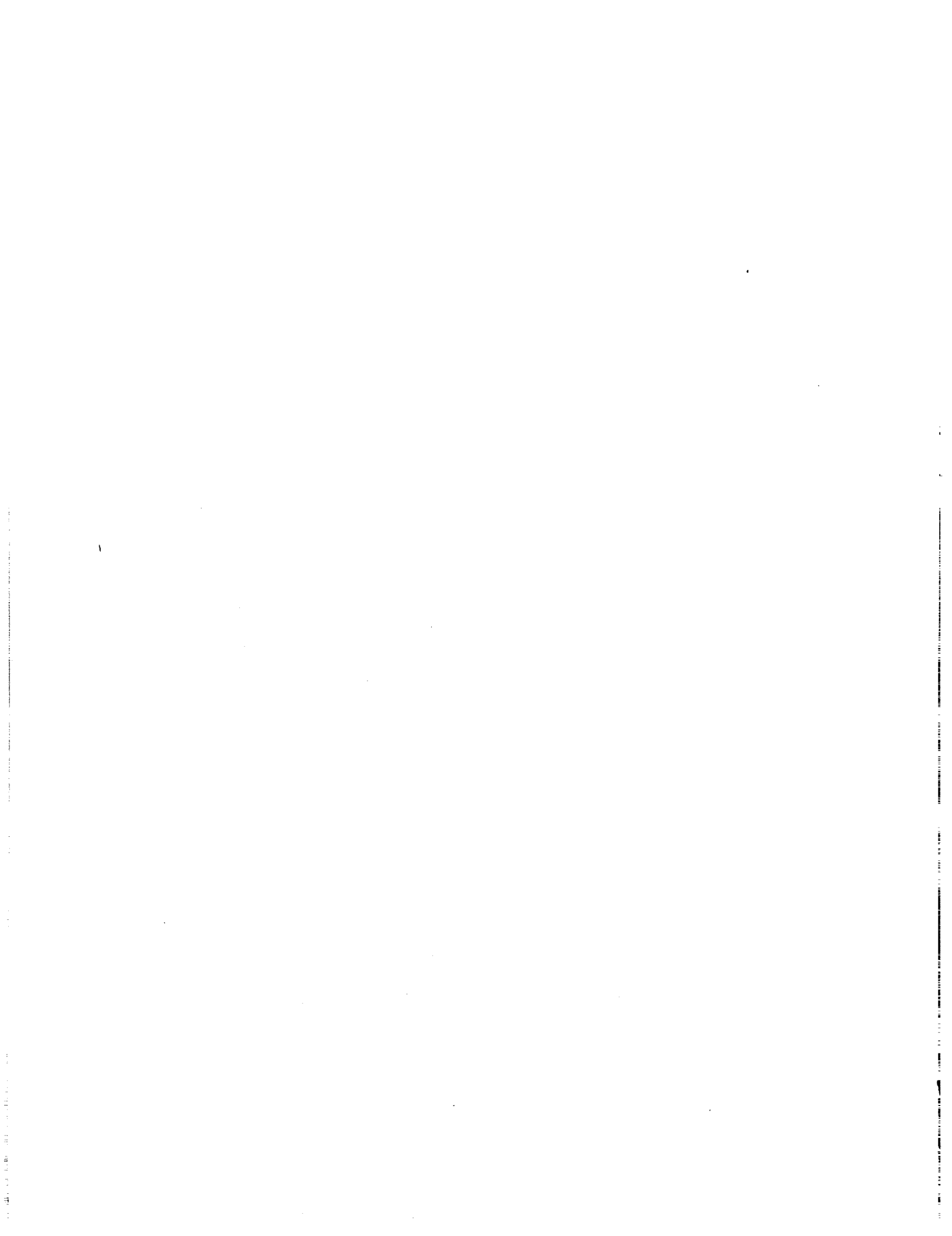


Figure 7. A schematic diagram for the procedure of flutter boundary prediction using the U-g method



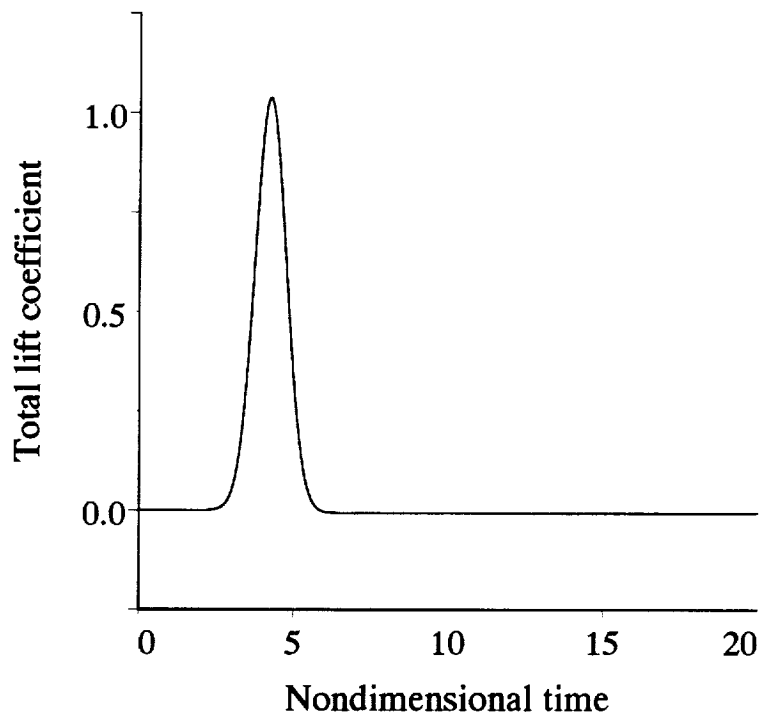


Figure 8. Time history of the total lift coefficient of the unswept rectangular wing with 6% thick circular-arc airfoil under a harmonic motion. ($M = 0.715$, angle of attack = 0.0 , Euler)

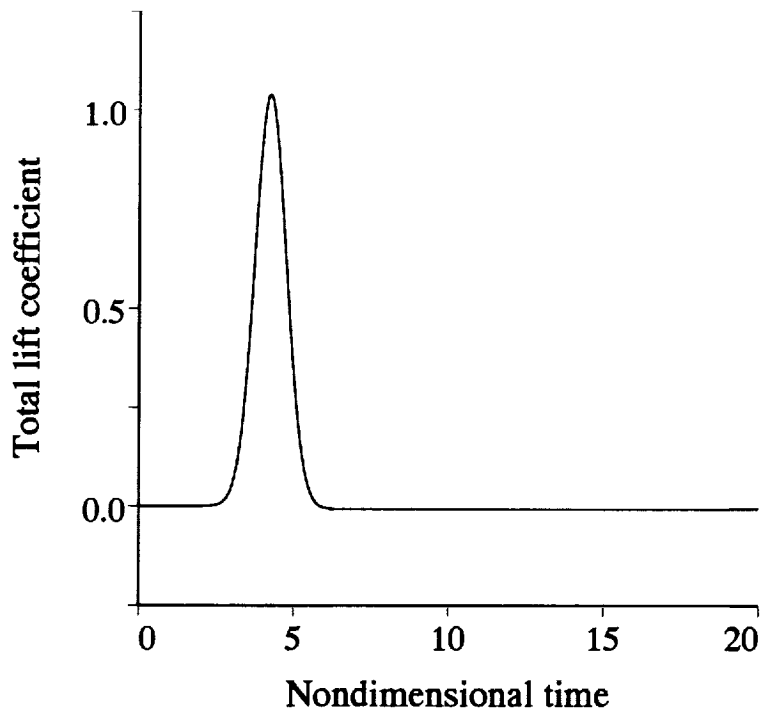


Figure 9. Time history of the total lift coefficient of the unswept rectangular wing with 6% thick circular-arc airfoil under a smoothly varying pulse motion. ($M = 0.715$, angle of attack = 0.0 , Euler)

ORIGINAL PAGE
COLOR PHOTOGRAPH

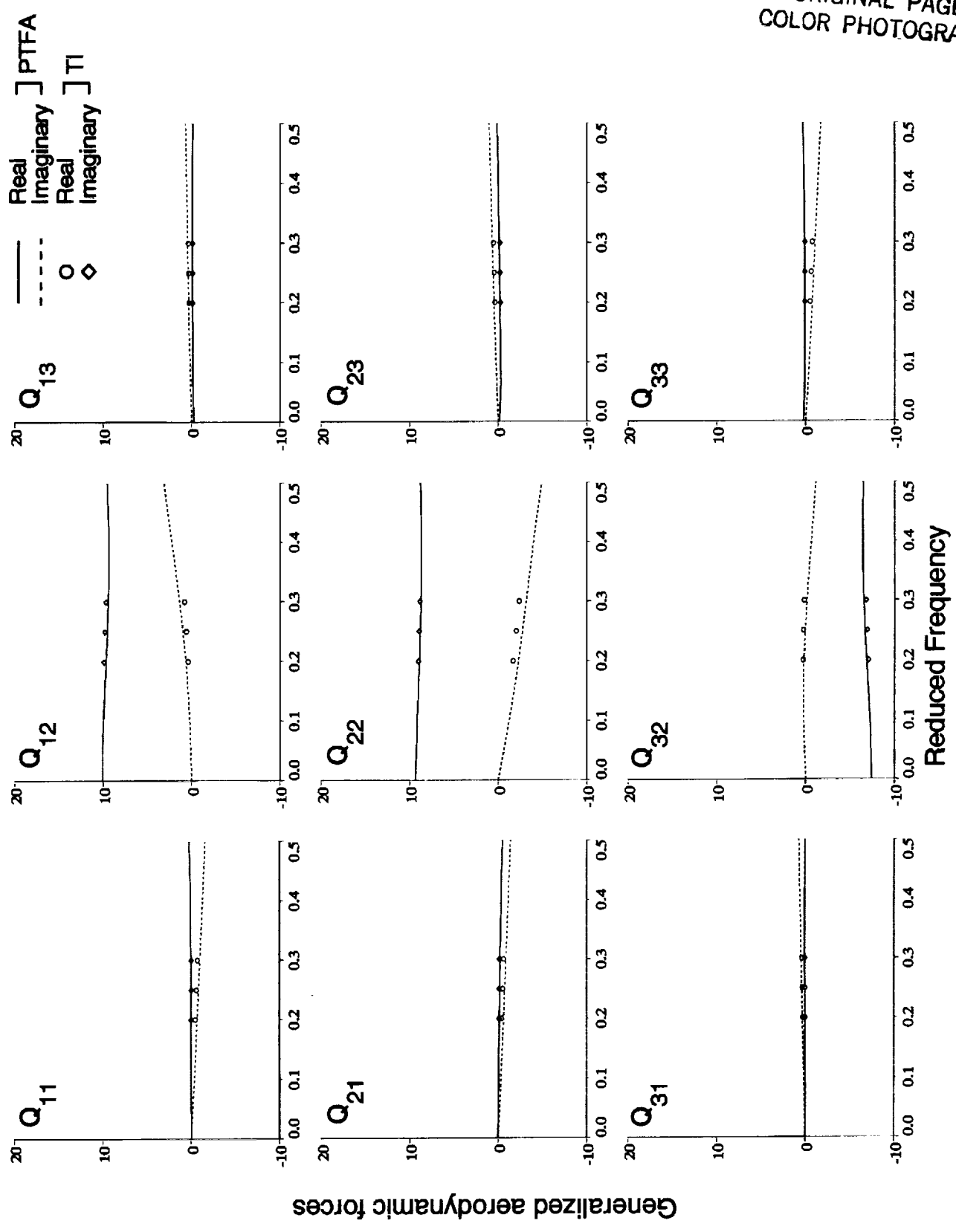
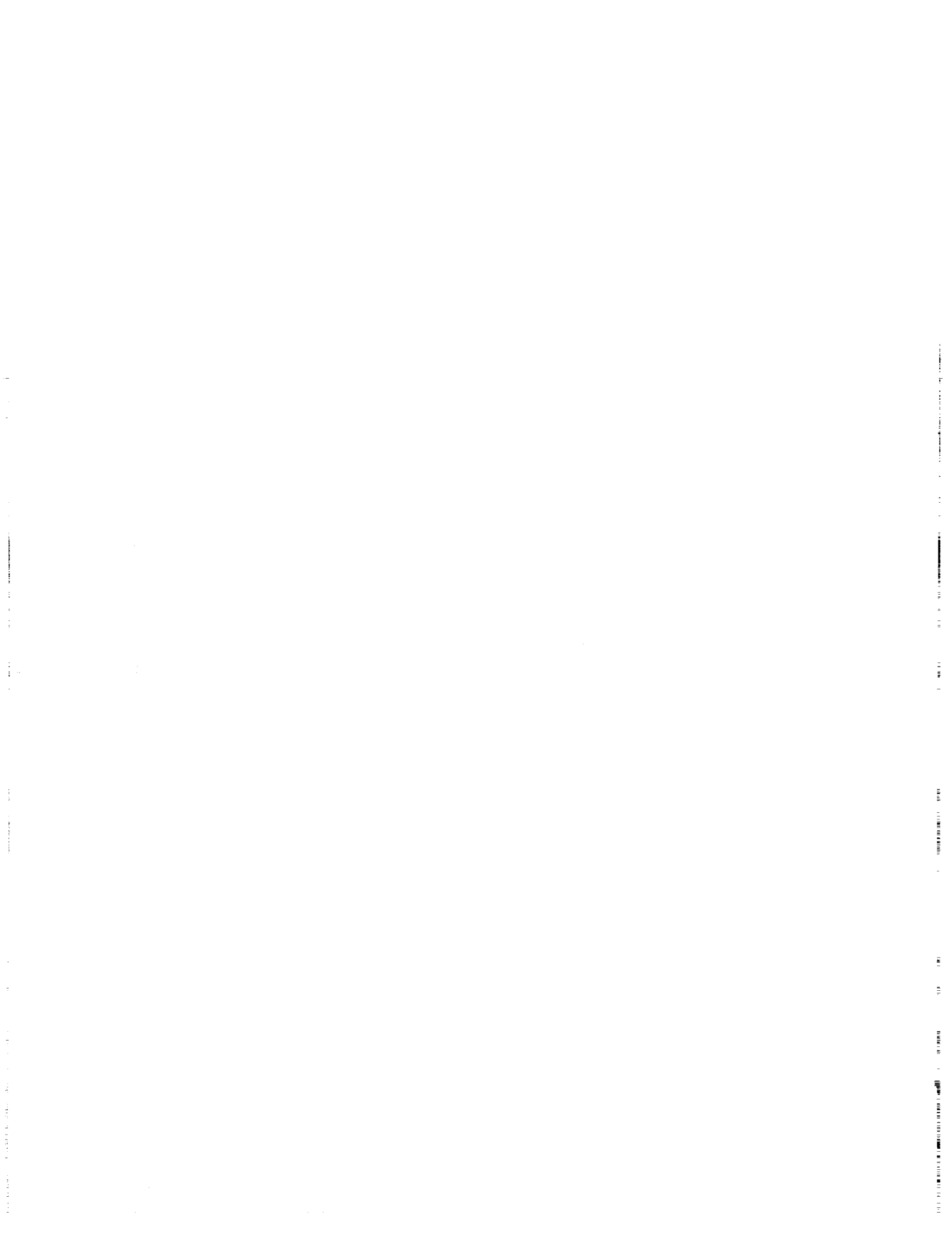


Figure 10. Comparison of generalized aerodynamic forces obtained by using the time integration and pulse transfer-function analysis methods. (Code : ENSAERO, Grid : 151x35x35)



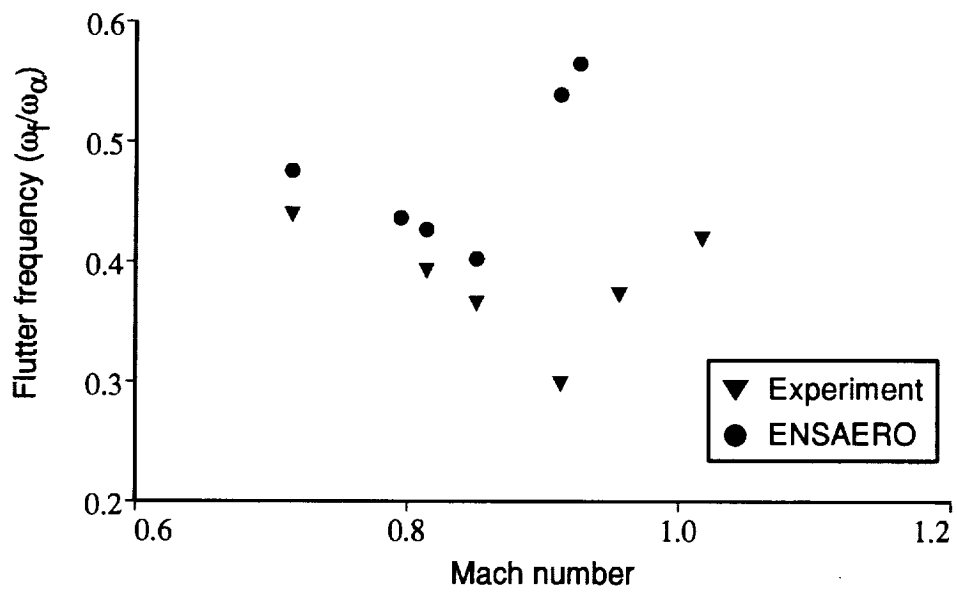


Figure 11. Comparison of the computed flutter frequency of a rectangular unswept wing with the experiment.

1
2
3
4
5
6
7
8
9
10
11
12
13
14
15
16
17
18
19
20
21
22
23
24
25
26
27
28
29
30
31
32
33
34
35
36
37
38
39
40
41
42
43
44
45
46
47
48
49
50
51
52
53
54
55
56
57
58
59
60
61
62
63
64
65
66
67
68
69
70
71
72
73
74
75
76
77
78
79
80
81
82
83
84
85
86
87
88
89
90
91
92
93
94
95
96
97
98
99
100

